Article

Calcium-dependent regulation of the cell cycle via a novel MAPK–NF-κB pathway in Swiss 3T3 cells

Violaine Sée, Nina K.M. Rajala, David G. Spiller, and Michael R.H. White

Centre for Cell Imaging, School of Biological Sciences, University of Liverpool, Liverpool L69 7ZB, England, UK

Nuclear factor kappa B (NF-κB) has been implicated in the regulation of cell proliferation and transformation. We investigated the role of the serum-induced intracellular calcium increase in the NF-κB–dependent cell cycle progression in Swiss 3T3 fibroblasts. Noninvasive photoactivation of a calcium chelator (Diazo-2) was used to specifically disrupt the transient rise in calcium induced by serum stimulation of starved Swiss 3T3 cells. The serum-induced intracellular calcium peak was essential for subsequent NF-κB activation (measured by real-time imaging of the dynamic p65 and IκBα fluorescent fusion proteins), cyclin D1 (CD1) promoter-directed transcription (measured by real-time luminescence imaging of CD1 promoter-directed firefly luciferase activity), and progression to cell division. We further showed that the serum-induced mitogen-activated protein kinase (MAPK) phosphorylation is calcium dependent. Inhibition of the MAPK- but not the PtdIns3K-dependent pathway inhibited NF-κB signaling, and further, CD1 transcription and cell cycle progression. These data suggest that a serum-dependent calcium signal regulates the cell cycle via a MAPK–NF-κB pathway in Swiss 3T3 cells.

Introduction

The nuclear factor kappa B (NF-κB)/Rel family of transcription factors consists of five members (p50, p52, p65/RelA, c-Rel, and RelB) that form a variety of homo- or heterodimeric complexes (Sen and Baltimore, 1986). NF-κB is activated by its release from cytoplasmic IκB proteins and subsequently translocates into the nucleus (Baeuerle and Baltimore, 1996; Baldwin, 1996). Activation is triggered by signal-induced phosphorylation of IκBs, which targets the inhibitors for rapid degradation by the proteasome (Thanos and Maniatis, 1995). Several papers have suggested a role for the NF-κB and IκB gene products in cell proliferation, transformation, and tumor development (Rayet and Gelinas, 1999; Chapman et al., 2002).

Cell cycle activation is in part coordinated by D-type cyclins, which are rate limiting and essential for the progression through the G1 phase of the cell cycle (Coqueret, 2002). Cyclin D1 (CD1) is expressed in most mammalian cells and varies in abundance during the cell cycle, peaking in mid-G1. The level of CD1 protein is largely controlled by the rate of CD1 gene transcription, which is regulated by multiple transcription factors. The CD1 promoter region includes binding sites for NF-κB (Guttridge et al., 1999; Hinz et al., 1999; Joyce et al., 1999), E2F/DP, sp-1/sp-3 (Watanabe et al., 1998), AP-1 (Lee et al., 1999), STAT (Matsumura et al., 1999) and CREB (Lee et al., 1999). NF-κB has been shown to control cell growth and differentiation through transcriptional regulation of CD1 (Guttridge et al., 1999; Hinz et al., 1999). A nuclear NF-κB like DNA-binding activity has been shown to be induced during the G0–G1 transition after serum stimulation in mouse fibroblasts (Baldwin et al., 1991). Despite the fact that the link between NF-κB and cell cycle progression is now (at least partly) established, the upstream events leading to NF-κB pathway activation upon growth factor stimulation remain to be elucidated.

Stimulation of quiescent cells with a variety of growth factors or mitogens induces a transient rise in the intracellular free calcium concentration ($[Ca^{2+}]_i$) through rapid mobilization from both inositol 1,4,5-triphosphate stores and from the cells' external environment (McNeil et al., 1985; Takuwa et al., 1995; Ichikawa and Kiyohara, 2001). Such papers have established clear evidence for a role of $[Ca^{2+}]_i$ in the G1/S and G2/M phases of the cell cycle (Takuwa et al., 1995; Cheng et al., 1996; Whitaker and Larman, 2001). However, there have been only a few reports suggesting an important role for $[Ca^{2+}]_i$ at the G0–G1 transition. Regulation of the

Abbreviations used in this paper: $[Ca^{2+}]_i$, intracellular free calcium concentration; CaMK, Ca-calmodulin kinase; CD1, cyclin D1; NF-κB, nuclear factor kappa B.

NF-κB pathway by $[Ca^{2+}]_i$ has been studied in several models, including T-cell stimulation (Truneh et al., 1985), B lymphocytes (Dolmetsch et al., 1998), and cerebellar granule neurons (Lilienbaum and Israel, 2003).

In the absence of growth factors, 3T3 fibroblasts enter the G0 quiescent state. The addition of growth factors initiates cells to enter the G1 phase of the cell cycle, the synthesis of DNA (S phase) and cell division (M phase) (Lau and Nathans, 1985; Bravo, 1990). During the G0–G1 transition, the expression of several transcription factors regulates cell growth and DNA synthesis. In most cell types, the mitogenic signal is relayed by the activation of the ubiquitously expressed p42/p44^{MAPK} (ERK1/ERK2) (Chen et al., 1992; Lenormand et al., 1993). Previous works have shown that sustained activation of p42/p44^{MAPK} is required for fibroblasts to pass the restriction point in G1 and enter S-phase (Pages et al., 1993; Brondello et al., 1995). The p42/p44^{MAPK} activity has been reported to be dependent on calcium concentration in a swine carotid artery model (Katoch et al., 1999). This might suggest that p42/p44^{MAPK} could have a role in cell cycle regulation downstream from the serum-induced calcium increase. The activation of p42/p44^{MAPK} results in the activation of a range of transcription factors, and CD1 expression is positively regulated by this p42/p44^{MAPK} signal (Lavoie et al., 1996).

A link between intracellular calcium increase, mitogenic activation, and NF-κB pathway activation has not previously been established. In the present work, we have applied flash photolysis of caged calcium chelator in living cells to study the precise role of calcium in CD1 gene transcription and subsequent cell proliferation after serum stimulation of serum-starved Swiss 3T3 fibroblasts. We have investigated the relationship between growth factor activation, $[Ca^{2+}]_i$ increase, MAPK and NF-κB activation, cell cycle gene transcription, and cell cycle progression. We report that serum stimulation of starved 3T3 fibroblasts induces a calcium-dependent increase in p42/p44^{MAPK} phosphorylation and NF-κB signaling, which in turn appears to activate CD1 gene transcription and cell cycle progression.

Results

Serum stimulation activates the NF-κB pathway and subsequent CD1 transcription

We investigated whether NF-κB regulates cell cycle entry and CD1 transcription in Swiss 3T3 cells. Serum starvation induced significant cell cycle arrest in 3T3 cells. 84% of cells were in G0/G1 phase and 11% in S-phase 24 h after serum starvation (Fig. 1 A). 18 h after serum stimulation, 44% of the cells were in S-phase. This indicated that, as expected, serum stimulation induced cell cycle progression in 3T3 cells. In the presence of an NF-κB inhibitor, Bay117082, only 23% of cells were found to be in S-phase 18 h after serum stimulation. Therefore, these data provided preliminary evidence that NF-κB activation is a key step for cell cycle progression in 3T3 fibroblasts.

To assess the role of NF-κB–dependent transcription in cell cycle progression, we transfected a reporter vector, which contained five copies of the NF-κB consensus binding site, in front of the firefly luciferase reporter gene. Then, we used noninvasive luminescence imaging to measure the time course of luciferase gene expression levels. We observed a peak of luminescence activity 7 h after serum stimulation (Fig. 1 B). When the same experiment was performed using the CD1 promoter (which contains three NF-κB binding sites; Hinz et al., 1999) upstream of the luciferase reporter gene, the luminescence activity reached a maximum at 3 h after serum stimulation (Fig. 1 B). A second peak of luminescence was also observed 20 h after serum stimulation, corresponding to the timing of cell division and the beginning of a new cell cycle. Analysis of endogenous CD1 mRNA levels by RT-PCR showed an accumulation of CD1 mRNA after 4 h, which reached a peak 8 h after serum stimulation (Fig. 1 C). This increase in CD1 mRNA was inhibited by the NF-κB inhibitor Bay117082 (Fig. 1 D). The serum-induced activation of CD1 promoter activity (at 6 h) was also inhibited by treatment with Bay117082 (Fig. 2 A). In order to provide further evidence for the direct role of NF-κB in serum-induced CD1 promoter activity, we studied the effect on coexpression with the CD1 promoter of either truncated IκBα (Fig. 2 A) or transdominant-negative IKKα or IKKβ (Fig. 2 B). Cotransfection with each of these expression vectors significantly repressed CD1 luciferase reporter activation, with the repression by the transdominant IKKβ expression being particularly strong.

In order to confirm the crucial role of the NF-κB pathway for serum induction of CD1 gene expression, we investigated deletion mutants of the CD1 promoter (Fig. 2, C and D). The −1745 CD1 promoter gave 1.9-fold ± 0.14 (SEM) induction in response to serum. A −963 CD1 promoter, which retained all three NF-κB sites, gave twofold ± 0.13 (SEM) induction. A −66 CD1 promoter, which had two NF-κB sites deleted, gave a significantly reduced serum response (1.4-fold ± 0.09; SEM). Most significantly, mutation of the remaining NF-κB site in the −66 construct further reduced the serum response (1.14-fold ± 0.09; SEM).

To investigate the mechanism by which serum stimulation activates the NF-κB signaling pathway, we made use of fluorescent fusion constructs expressing the p65 Rel/NF-κB protein and the inhibitor IκBα (Nelson et al., 2002a). We monitored p65-dsRed translocation into the nucleus and IκBα-EGFP degradation in living cells by using time-lapse confocal microscopy at 2-min intervals. p65-dsRed was found to translocate into the nucleus and reached a peak nuclear concentration 25 min after serum stimulation (Fig. 3, A and B; Video 1, available at http://www.jcb.org/cgi/content/full/jcb.200402136/DC1). IκBα was found to be completely degraded after 15 min. The same timing of movement and degradation was also observed in experiments to study the endogenous p65 and IκBα proteins using Western blotting (Fig. 3 C) on nuclear extracts (for p65) and whole-cell extracts (for IκBα). Therefore, these data suggested that the fluorescent fusion proteins faithfully reported the dynamics of the endogenous p65 and IκBα response to serum in 3T3 cells.

Intracellular calcium rise is required, but not sufficient for serum-induced NF-κB activity

Calcium is a major second messenger that is activated during the cell cycle and by growth factor stimulation (Means, 1994; Santella, 1998; Ichikawa and Kiyohara, 2001). We investigated how serum stimulation modulates $[Ca^{2+}]_i$ by
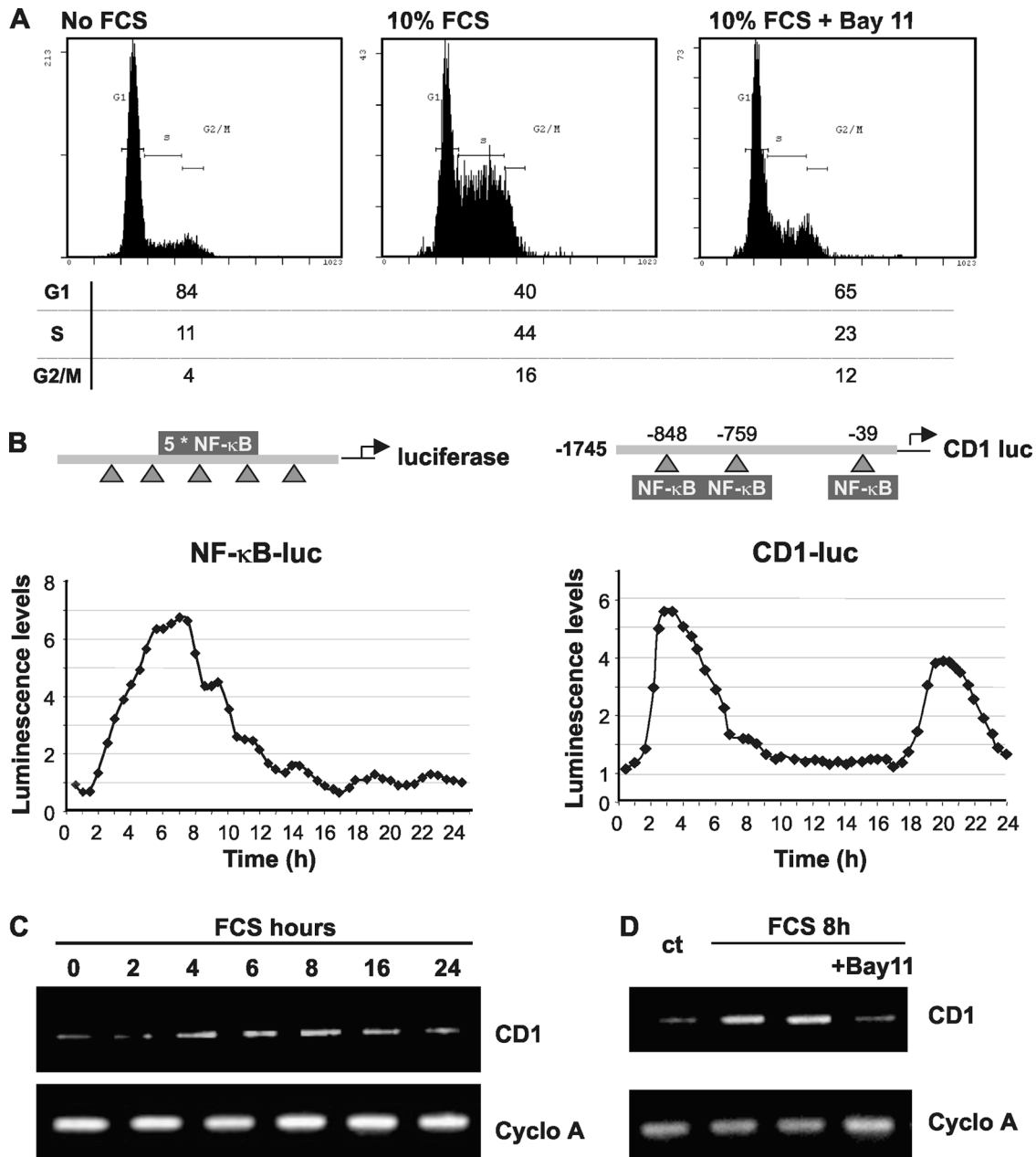
Figure 1. **NF-κB dependent transcription is essential for cell cycle progression.** (A) Swiss 3T3 fibroblasts were serum starved for 24 h. They were then stimulated with 10% FCS for 18 h in the absence or presence of an NF-κB inhibitor (5 μM Bay117082). Cell cycle stage was determined by flow cytometry analysis of propidium iodide–stained cells. (B) Swiss 3T3 cells were transfected with the indicated reporter vectors (NF-κB luc and −1745 CD1-luc). 24 h after serum starvation, firefly luciferin (Biosynth) was added to the medium (0.5-mM final concentration). 2 h later, serum stimulation was performed and luminescence imaging was carried out using a Hamamatsu 4880-65 liquid nitrogen–cooled CCD camera. Images were acquired using 30-min integration times. (C) RT-PCR analysis was performed using primers specific to CD1 or cyclophilin A (control), with total RNA prepared from cells stimulated with 10% FCS at indicated time points. (D) RT-PCR analysis, with total RNA prepared from nonstimulated starved cells (ct) or cells stimulated 8 h with 10% FCS in the presence or absence of Bay117082.

loading the cell-permeant fluorescent dye Fluo-4-AM. Serum induced an immediate and significant peak in $[Ca^{2+}]_i$ (Fig. 4 A). The transient increase in $[Ca^{2+}]_i$ started 1 s after serum stimulation and lasted for 30 s. No further oscillations of $[Ca^{2+}]_i$ were observed (over 5 min; unpublished data). We used a calcium chelator (BAPTA-AM) to investigate the effect of ablation of the serum-induced calcium signal on p65-dsRed translocation. 10 μM BAPTA-AM was loaded into the cells for 20 min and the cells were then stimulated

with 10% serum. Treatment with the calcium chelator led to a drastic inhibition in the level of p65 translocation in comparison to control cells (Fig. 4 B). The ratio of the nuclear/cytoplasmic fluorescence intensities reached a maximum of 1.6 in control conditions versus 0.4 in presence of BAPTA.

BAPTA can inhibit many calcium-dependent events in cells, leading to nonspecific toxicity after 4 h. To be able to study the long-term role of the serum-induced $[Ca^{2+}]_i$ increase, we developed a noninvasive method to abolish the
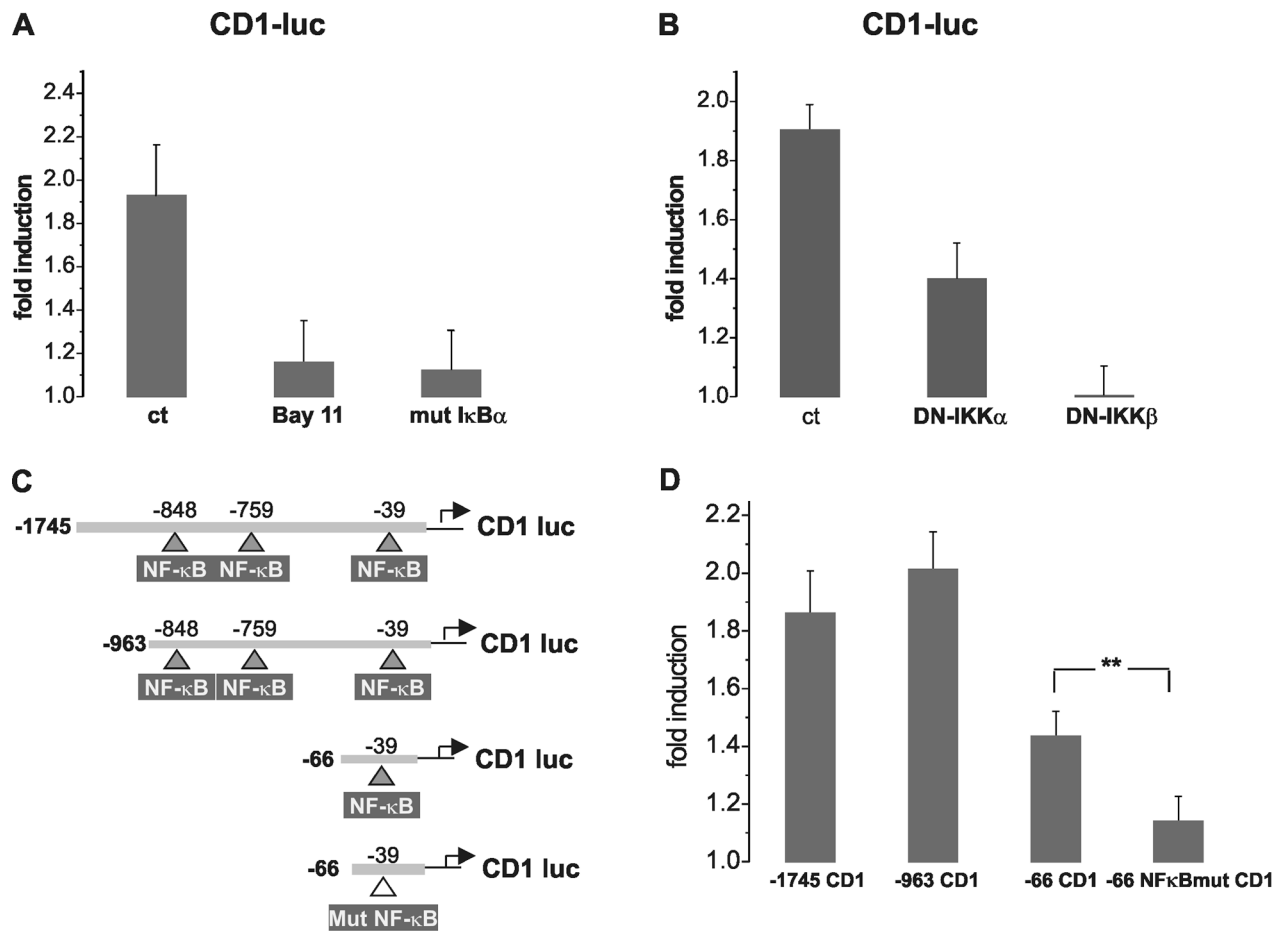
A CD1-luc

B CD1-luc

C

D

Figure 2. **The induction of CD1 promoter activity by serum is NF-κB dependent.** (A) Cells were transfected with the CD1 reporter vector. After a period of 24 h of serum starvation, cells were stimulated or not (ct) with 10% FCS in the absence (ct) or presence of an NF-κB inhibitor (5 μM Bay117082; 20 min preincubation), or were cotransfected with a truncated active mutant of IκBα. (B) Cells were cotransfected with the CD1 reporter vector and either a control empty vector, or a vector expressing either transdominant-negative IKKα or IKKβ. (C) Schematic diagrams of the several CD1-luciferase reporters used. (D) Cells were transfected with the indicated reporters. (A, B, and D) Results are expressed as fold activation relative to the level measured in nonstimulated starved cells. Cells were assayed for luciferase activity 6 h after serum stimulation. Histograms are means ± SEM of triplicate values. Each experiment was performed three times. **, ($P < 0.05$) indicates statistically significant difference (two-tailed t test).

calcium increase, based on photoactivation of the caged calcium scavenger Diazo-2, which displays a low affinity for Ca^{2+} before photolysis. This affinity is increased 30-fold after illumination at 360 nm. Diazo-2 was loaded into 3T3 cells that were then subjected to a brief (10 s) period of photoactivation. This photoactivation alone induced a transient 20% decrease in $[Ca^{2+}]_i$ levels (Fig. 5 A). No significant decrease in $[Ca^{2+}]_i$ occurred in cells that were loaded with Diazo-2 but were not illuminated, nor in cells that were illuminated but not loaded with Diazo-2 (unpublished data). Experiments where illumination was performed immediately after serum induction showed that the photolysis of Diazo-2 inhibited the serum-induced calcium peak (Fig. 5 B), but had no effect on subsequent intracellular calcium levels. Photoactivation of Diazo-2 after serum stimulation also blocked detectable p65 translocation into the nucleus (Fig. 5 C) as well as NF-κB–dependent gene transcription from the NF-κB consensus and CD1 promoters (threefold decrease; Fig. 5 D). For all these experiments, the control cells shown were the nonilluminated fields from the same illuminated experi-

ment. Additional controls (analyzing the effects of serum stimulation on illuminated cells that were not previously loaded with Diazo-2) were also performed to ensure that the lack of translocation and transcription was not due to illumination, UV-toxicity, or free radical production. These control experiments gave identical results to the nonilluminated cells with respect to p65 translocation and reporter luminescence (unpublished data). Additionally, we also analyzed the effects of serum on cells that were loaded with Diazo-2 and subjected to photoactivation 5 min before serum stimulation (Fig. S1, available at http://www.jcb.org/cgi/content/full/jcb.200402136/DC1). In this important control experiment, the calcium response of the cells to the serum stimulation was identical to the usual response that was obtained in the absence of previous uncaging. Furthermore, the NF-κB translocation and NF-κB–Luc responses to serum were unaffected by the uncaging procedure (Fig. S1).

To further characterize the relationship between the transient $[Ca^{2+}]_i$ increase and subsequent p65 activation, we performed the same experiment using flash photolysis with a
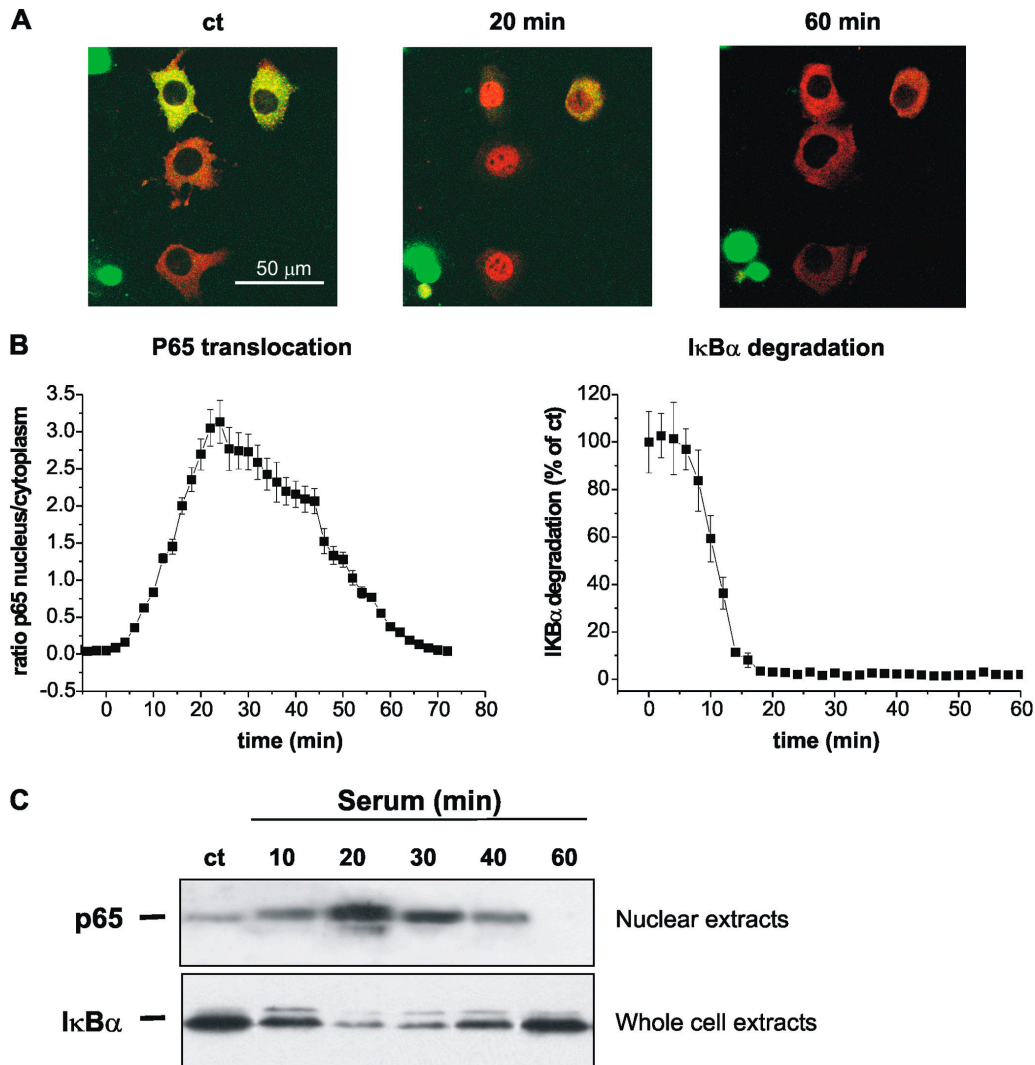
A

ct   20 min   60 min

B

P65 translocation

IκBα degradation

C

Serum (min)

Figure 3.   **Serum stimulation promotes p65 translocation into the nucleus as well as IκBα degradation.** (A) p65-dsRed (red staining) and IκBα-EGFP (green staining) were cotransfected into Swiss 3T3 fibroblasts. 24 h after serum starvation, the cells were stimulated with 10% FCS. Confocal images were collected every 2 min from transfected living cells cultured in a humidified CO_2 incubator (5% CO_2, 37°C) (Video 1, available at http://www.jcb.org/cgi/content/full/jcb.200402136/DC1). (B) Mean fluorescence intensities were measured for each time point in both the nucleus and cytoplasm for p65-dsRed, and the results are shown as a ratio. The IκBα-EGFP mean fluorescence intensities were measured at each time point in the cytoplasm alone and the results presented as the relative intensity to the starting fluorescence levels. Experiments were performed at least four times, with four fields. In each field there were typically 3–4 transfected cells. (C) Endogenous p65 levels in the nucleus were assessed after 10% FCS stimulation for the indicated time by Western blotting nuclear extracts using an anti-p65 antibody (1:1,000). Endogenous IκBα was assessed in whole-cell extracts using an anti-IκBα antibody (1:1,000).

caged calcium donor. Photoactivation of NP-EGTA induced a 22% transient increase above the resting level in $[Ca^{2+}]_i$ (Fig. 6 A). This increase was smaller, but of the same magnitude to that obtained with serum stimulation (22% with illumination compared to 60% above the resting level with serum). The increase in $[Ca^{2+}]_i$ after illumination lasted for a similar duration to that obtained with serum stimulation (∼20 s). Despite the similar dynamics in $[Ca^{2+}]_i$ levels (compared to serum stimulation), the illumination of NP-EGTA was unable to induce any detectable p65 translocation (Fig. 6 B). Together, these data (Fig. 5 and Fig. 6) suggest that p65 translocation and downstream regulation of gene transcription is dependent on a transient increase of $[Ca^{2+}]_i$. However, that increase alone, without the presence of other serum-dependent signals, was not sufficient to activate p65. Therefore, we next set out to investigate which other factor(s) upstream of IκBα degradation were activated by growth factors and were dependent on calcium signaling.

Serum-induced NF-κB activity is dependent on calcium-sensitive p42/p44^{MAPK} activity

Candidate signaling enzymes that might be involved in the serum-induced NF-κB activity were p42/p44^{MAPK} and Akt, which are known to be activated during cell proliferation (Pages et al., 1993; Davies et al., 1999), and have been reported to regulate the IκB/NF-κB signaling pathway (Romashkova and Makarov, 1999; Madrid et al., 2001). Other candidates were investigated including Ca-calmodulin kinases (CaMKs), calcineurin, and calmodulin. Inhibition of these either had no significant effect (cyclosporin A and
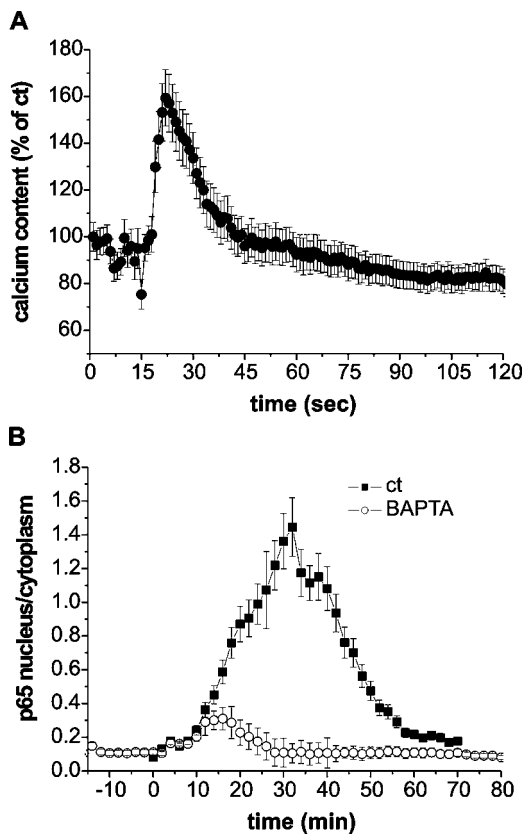
A

B

Figure 4. **Serum-induced p65 translocation into the nucleus is [Ca²⁺]ᵢ dependent.** (A) Starved cells were loaded with 1 μM Fluo-4-AM for 20 min at 37°C and intracellular calcium changes were recorded using laser scanning confocal microscopy (488-nm excitation, 505–550-nm emission) in response to serum. Images were taken every second for 2 min, and the increase of fluorescence was calculated taking level in the control unstimulated cells as 100%. (B) Swiss 3T3 cells were transfected with p65-dsRed. Confocal images were obtained and analyzed as described above. 24 h after serum starvation, the cells were either stimulated with serum alone (filled squares) or pretreated for 10 min with 10 μM BAPTA-AM (open circles). Experiments were performed at least four times, with four fields. In each field there were typically 3–4 transfected cells.

KN93; Fig. S2, available at http://www.jcb.org/cgi/content/full/jcb.200402136/DC1) or inconclusive effects (calmidazolium; unpublished data). We measured IκBα degradation (by Western blotting) after a 20-min pretreatment with either the calcium chelator BAPTA-AM, the MAPK kinase (MEK) inhibitor PD98059, or the PtdIns3k inhibitor wortmannin. IκBα degradation was completely inhibited by PD98059 (Fig. 7 A). A similar level of inhibition also occurred in the presence of BAPTA-AM. However, wortmannin had no effect on IκBα degradation, suggesting that IκBα degradation was calcium- and MAPK-dependent, but not PtdIns3k dependent. When the inhibitors were applied together, no additive effect was observed. Measurement of IκBα degradation and p65 translocation by confocal microscopy of the fluorescent fusion proteins further revealed that IκBα degradation was delayed and strongly reduced in presence of PD98059 (50% of IκBα remained versus 10% in control cells, 100 min after serum stimulation; Fig. S4, available at http://www.jcb.org/cgi/content/full/jcb.200402136/

DC1). The consequent p65 translocation was also abolished in the presence of PD98059 (Fig. S4).

We further investigated both MAPK and Akt activity using antibodies directed against phosphorylated p42/p44^MAPK (Thr185/202/Tyr185/204) and phospho-Akt (Ser 473). These enzymes were found to be activated by a 10-min serum stimulation. p42/p44^MAPK activity was inhibited (as expected) by PD98059, and more significantly was also inhibited by BAPTA-AM. However, p42/p44^MAPK activity was not sensitive to wortmannin. Akt activity was inhibited by all three inhibitors tested (Fig. 7 A). These data support the hypothesis that IκBα degradation is dependent on increases in p42/p44^MAPK activity and that this activity is itself dependent on [Ca²⁺]ᵢ. However, IκBα degradation was not dependent on PtdIns3k activity, which therefore appeared to act downstream from the [Ca²⁺]ᵢ increase and MAPK activation.

Next, we investigated the order and timing of MAPK and Akt activation after serum stimulation (by Western blotting; Fig. 7 B). The phosphorylation of p42/p44^MAPK was detected as early as 2 min and was complete after 5 min of serum stimulation. In contrast, Akt was weakly phosphorylated after 5 min, and reached a maximum after 10 min. These data can be compared to the previous observations that IκBα was degraded after 10 min (Fig. 3 B) and that p42/p44^MAPK activity was sensitive to [Ca²⁺]ᵢ, which reached a peak much earlier (1 min after stimulation; Fig. 4 A). Therefore, they suggest an upstream role for MAPK in IκBα degradation.

The key role of p42/p44^MAPK in NF-κB-dependent cell cycle progression was further investigated by studying its role in gene transcription and cell cycle progression. We tested the effects of both PD98059 and wortmannin on consensus NF-κB and CD1 promoter activity. PD98059 was found to block the serum-induced NF-κB–Luc and CD1-Luc reporter activity (Fig. 8 A), whereas the PtdIns3k inhibitor wortmannin gave rise to only weak inhibition of gene expression. The effect on cell cycle progression was further investigated by flow cytometer analysis. In the presence of the MEK inhibitor PD98059, 22% of cells were found to be in S-phase after 18 h serum stimulation, compared to the control without inhibitor, where 46% of cells were in S-phase (Fig. 8 B). These data support the concept that p42/p44^MAPK is a key regulator of NF-κB–dependent gene transcription (specifically CD1 transcription) and subsequent cell cycle progression.

Discussion

Rel/NF-κB proteins have been shown to participate in cellular growth control and neoplasia (for review see Gilmore, 1999), and many tumor cells display constitutively high levels of nuclear NF-κB activity (Barth et al., 1998; Brownell et al., 1988). The aim of the present work was to identify the mechanism by which the NF-κB pathway is activated during cell cycle commitment. First, we demonstrated the essential role of NF-κB in Swiss 3T3 cell cycle progression by inhibiting the NF-κB pathway with a pharmacological inhibitor that blocked the cell cycle in G1 phase. This is in line with one previous report (Hinz et al., 1999) where the cell
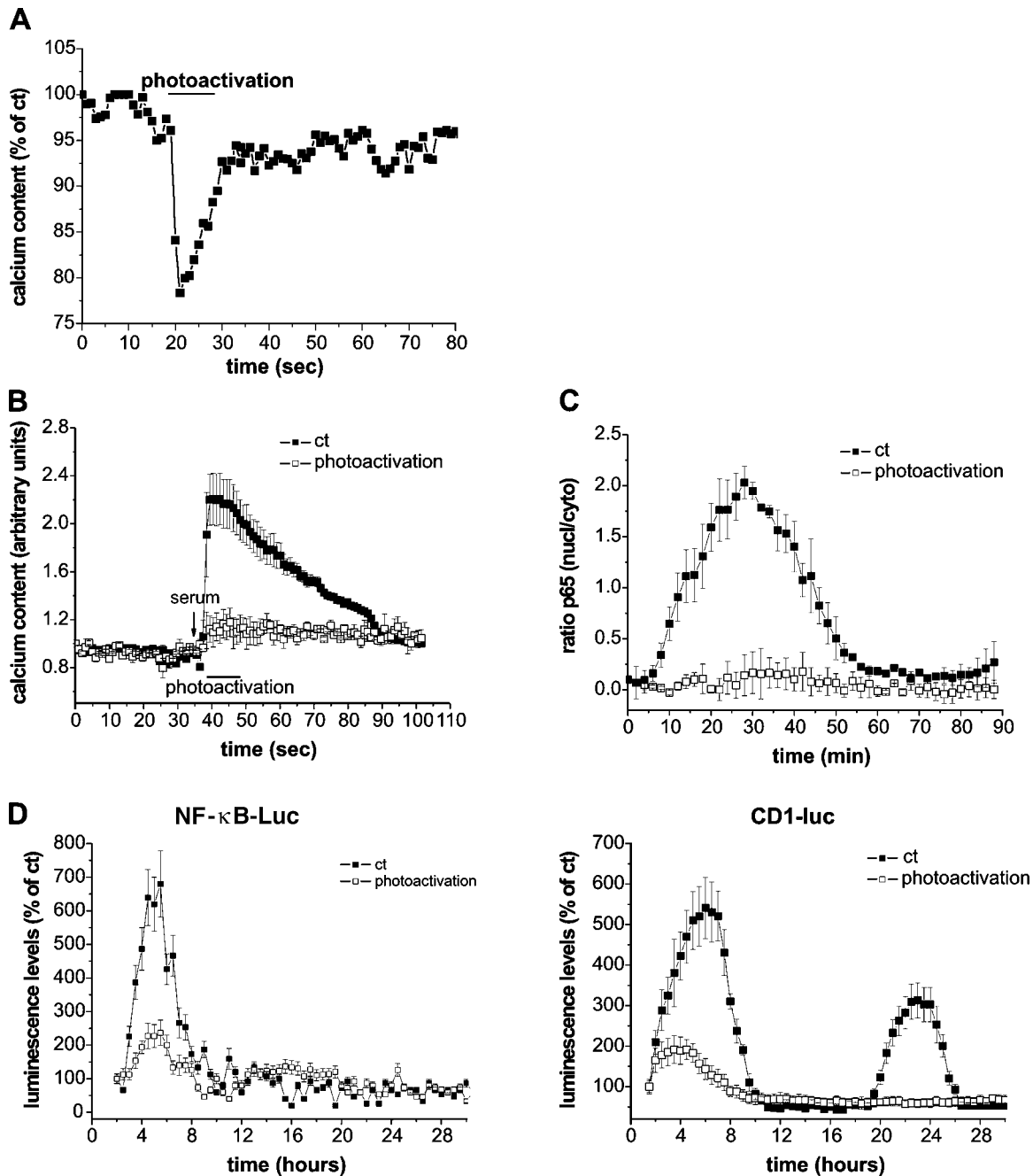
Figure 5. **The serum-induced [Ca^{2+}]$_i$ peak is essential for NF-κB–dependent signaling.** (A) Starved cells were loaded with both 0.6 μM Diazo-2 and 0.6 μM Fluo-4 for 20 min at 37°C. For uncaging Diazo-2, cells were illuminated for 10 s with a Micro-point photoactivation system (Photonic Instruments). Intracellular calcium content was monitored every second by confocal microscopy (488-nm excitation, 505–550-nm emission) of Fluo-4 fluorescence. (B–D) Swiss 3T3 cells were plated on a marked dish and transfected with 0.5 μg p65-dsRed and 1.5 μg of the reporter NF-κB–luc. After 24 h of serum starvation, the cells were loaded with both Fluo-4 and Diazo-2 as previously described. After one wash, the cells were stimulated with 10% FCS. 1 s later the cells were either illuminated for 10 s (open squares) or untreated (ct, filled squares). (B) Confocal microscopy was used as previously described to measure calcium content every second for 2 min. (C) p65 localization was assessed every 2 min for 90 min as already described. (D) An intensified CCD camera (VIM; Hamamatsu Corporation) was used to assess the luminescence from fields of individual control or photoactivated cells as previously described. Experiments were performed at least four times, with four fields. In each field there were typically 3–4 transfected cells. The horizontal line in A and B marks the period of photoactivation.

cycle kinetics were significantly affected by stable transfection of an expression vector for DA-IκBα.

We confirmed the previously identified role of NF-κB in regulation of CD1 transcription (Fig. 1; Guttridge et al., 1999; Hinz et al., 1999). The use of luminescence imaging with a highly sensitive CCD camera allowed us to follow

CD1 and consensus NF-κB promoter activities throughout the cell cycle. We observed two peaks of CD1 promoter activity within a 20-h interval, which appeared to correspond to the completion of one cell cycle. The NF-κB vector only showed one luminescence peak after serum stimulation, apparently indicating that the increase in NF-κB activity only
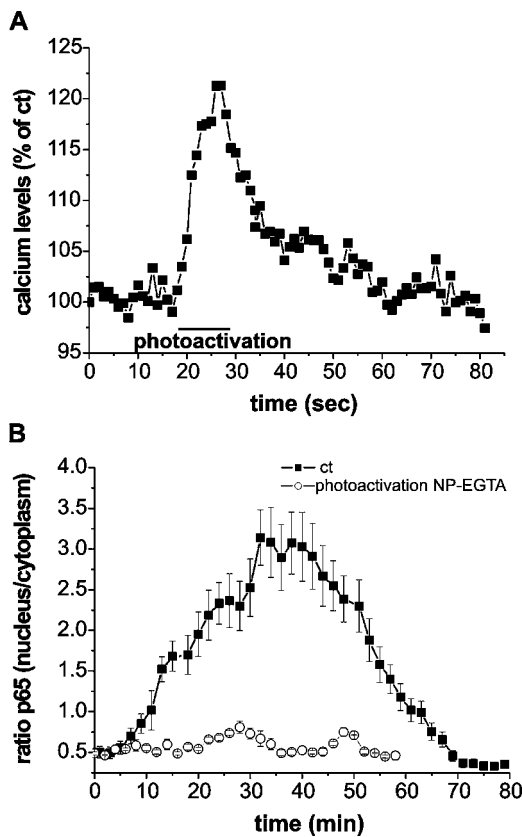
A

B

Figure 6. **A photoactivated induced $[Ca^{2+}]_i$ peak is not sufficient to promote p65 translocation.** (A) Starved cells were loaded with both 0.6 μM NP-EGTA and 0.6 μM Fluo-4 for 20 min at 37°C. For uncaging of NP-EGTA, cells were illuminated for 10 s with a Micro-point photo-activation system (Photonic Instruments). Intracellular calcium content was monitored every second by confocal microscopy (488-nm excitation, 505–550-nm emission) of Fluo-4 fluorescence. (B) Subsequently, p65 localization was assessed every 2 min for 90 min as already described. The control (ct) is nonilluminated cells stimulated with serum. Experiments were performed at least four times, with four fields. In each field there were typically 3–4 transfected cells. The horizontal line in A and B marks the period of photoactivation.

A

B

Figure 7. **IκBα degradation is both $[Ca^{2+}]_i$ and p42/p44^{MAPK} activity dependent.** (A) IκBα degradation, p42/p44^{MAPK} phosphorylation, and Akt phosphorylation were determined by Western blotting after 10 min of serum stimulation, using antibodies directed against IκBα (1:1,000), phospho-p42/p44^{MAPK} (Thr185/202/Tyr185/204; 1:5,000), and phospho-Akt (Ser 473; 1:5,000) and actin (1:10,000). Swiss 3T3 fibroblasts were serum starved for 24 h before serum stimulation, and the pharmacological inhibitors were added, where indicated, 20 min before the serum stimulation at the following concentrations: PD98059, 50 μM; BAPTA-AM, 10 μM; wortmannin, 100 nM. (B) The kinetics of p42/p44^{MAPK} and Akt activation were determined by Western blotting using anti-phospho-p42/p44^{MAPK} and anti-phospho-Akt antibodies. 24-h serum-starved 3T3 cells were stimulated by 10% FCS for indicated time points before cell lysis.

occurred in the first few hours after serum stimulation (i.e., at the G0–G1 transition). The small difference in timing observed in the dynamics of the NF-κB–luc and CD1-luc activity (peak of activity at 7 and 3 h, respectively) was presumably due to the contribution of other transcription factors to the activity of the CD1 promoter. The timing of NF-κB activity agreed with a previous report of DNA-binding kinetics (Baldwin et al., 1991). Therefore, these data were consistent with the hypothesis that NF-κB plays an important role in the early G0/G1 stage of the cell cycle. Further evidence for the role of NF-κB in the regulation of CD1 transcription in response to serum was obtained from deletion and mutation of the NF-κB sites in the CD1 promoter, which was found to reduce serum activation, identifying the key role for these elements in this process. Further evidence was obtained from overexpression of a truncated IKBα or transdominant-negative IKKα and β proteins (Fig. 2 B). IKKα has recently been shown to activate transcription of CD1 via direct activation of Tcf in mouse embryo fibroblasts upon serum stimulation (Albanese et al., 2003). In the absence of IKKα (IKKα$^{-/-}$
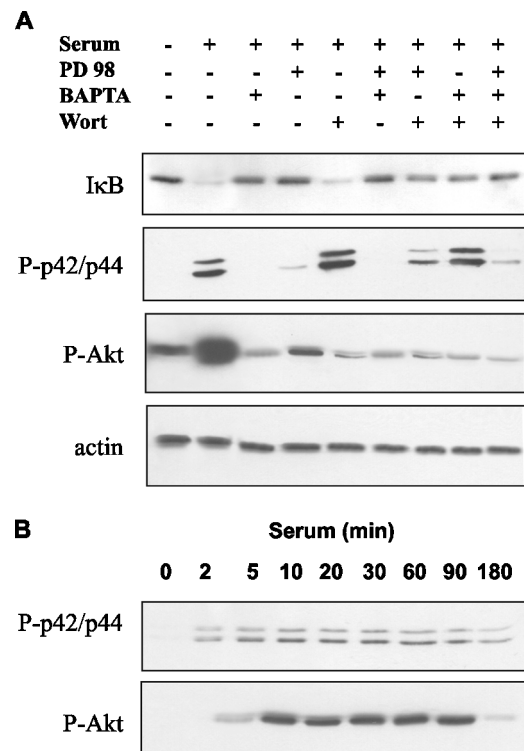
cells) the CD1 induction was delayed by about 3 h, perhaps suggesting an upstream reinforcement mechanism by IKKα to the control of the CD1 promoter. We used siRNA ablation of p65 to attempt to show the importance of this factor for CD1 transcription. However, we did not see any significant affect on CD1 transcription (Fig. S3, available at http://www.jcb.org/cgi/content/full/jcb.200402136/DC1). Despite good knock-down of this stable protein at the mRNA and protein levels, some protein remained, and therefore we cannot exclude the possibility that this was sufficient for function. It has also been shown that other NF-κB family members can activate the CD1 promoter (Guttridge et al., 1999; Westerheide et al., 2001; Rocha et al., 2003; Romieu-Mourez et al., 2003), and indeed the evidence for a critical role for p65 is therefore lacking.

In the present work, we have also shown the essential role of MAPK activity in cell cycle progression (Fig. 8 B) because inhibition of MAPK activity with PD 98059 blocked entry into the S-phase of the cell cycle. We observed a persistent p42/p44^{MAPK} activity upon serum stimulation (at least 3 h; Fig. 8 B), which appeared to be causally related to CD1 tran-
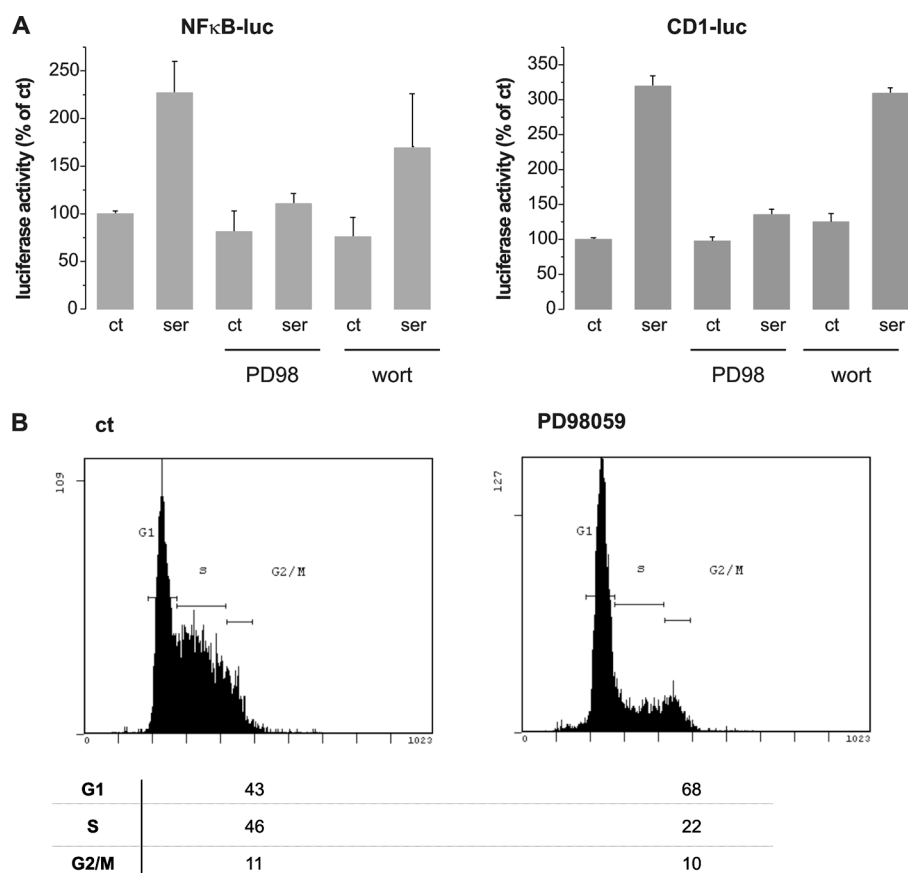
A

B

	ct	PD98059
G1	43	68
S	46	22
G2/M	11	10

Figure 8. **p42/p44^MAPK activation is determinant for CD1 transcription and further cell cycle progression.** (A) Swiss 3T3 cells were transfected with the indicated reporter vectors (NF-κB luc and −1745 CD1-luc). 24 h after serum starvation, cells were stimulated or not (ct) with 10% FCS in the absence or presence of MAPK inhibitor (PD98059, 50 μM; 20-min preincubation) or Akt inhibitor (100 nM wortmannin, 20-min preincubation) as indicated. 6 h after serum stimulation, in vitro luciferase activity was measured. Histograms are means ± SEM of triplicate values. Each experiment was performed three times. (B) Swiss 3T3 fibroblasts were serum starved for 24 h. 24 h after serum starvation, the cells were stimulated with 10% FCS for 18 h in the absence (ct) or presence of PD98059 (50 μM, 20-min preincubation). Cell cycle stage was determined by flow cytometric DNA histogram analysis of propidium iodide–stained cells.

scription (Fig. 8 A). Ryan et al. (2000) showed that p53-induced NF-κB activation can be mediated by MEK1 and pp90^rsk, suggesting that MAPK signaling can directly regulate NF-κB. Madrid et al. (2001) also reported regulation of IKK through p38 after IL-1β stimulation. However, it is unlikely that p38 activity has this role in serum stimulation because p38 is known to be an inhibitor of CD1 and cell cycle progression (Lavoie et al., 1996). Therefore, we concentrated on p42/p44^MAPK, which has been widely reported to be critical for cell cycle commitment. Our results suggest that p42/p44^MAPK activity is an early event (2 min) after serum stimulation and that it is critical for IKK phosphorylation (Fig. S4), IκBα phosphorylation (Fig. S4), and degradation (Fig. 7A; Fig. S4), and for NF-κB activation (Fig. S4) and CD1 transcription (Fig. 8 A). These observations establish for the first time a clear link between mitogenic MAPK signaling, NF-κB, CD1 transcription, and cell cycle commitment.

We investigated whether there was a link between PtdIns3K/Akt, the NF-κB pathway, and cell cycle commitment in fibroblasts stimulated by serum. A significant number of previous papers have reported a link between Akt and NF-κB (Ozes et al., 1999; Madrid et al., 2001; Meng et al., 2002). However, there remains considerable controversy about the position of Akt in the pathway and whether it lies upstream or downstream of the NF-κB activity. Some reports have indicated that Akt has a functional role upstream of NF-κB and induces its activity upon TNFα stimulation (Ozes et al., 1999) or PDGF stimulation (Romashkova and Makarov, 1999). Our results do not agree with these previous reports because wortmannin does not inhibit IκBα degradation

(even though Western blots confirm effective Akt inhibition by this agent; see Fig. 7 A). A further paper by Meng et al. (2002) reported that Akt could be a downstream target of NF-κB when the NF-κB pathway was activated by TNFα and lipopolysaccharides in NIH 3T3 cells. The determination of the exact position of Akt in this pathway was beyond the objectives of this work, yet our results support a parallel or a downstream role for Akt because the first time point of detectable Akt activation was at 10 min; the same time at which the IκBα degradation was observed. Moreover, Akt was found to be dependent on MAPK activity, but MAPK activity was independent of Akt activation (Fig. 7). We further investigated the role of Akt and MAPK on NF-κB–dependent transcription and CD1 promoter activity. MAPK inhibition strongly blocked CD1 and consensus NF-κB promoter activity, strengthening the case for an essential upstream role for MAPK signaling (Fig. 8 A). In a significant addition to previous reports (Lavoie et al., 1996), we demonstrated for the first time that this MAPK-dependent CD1 promoter activity occurs through the NF-κB pathway. The absence of any effect of wortmannin on CD1 promoter activity conflicts with a paper by Albanese et al. (2003), who reported an inhibitory effect of another PtdIns3K inhibitor, LY294002, on CD1 transcription and expression in mouse embryonic fibroblasts.

We also showed the critical role of calcium signaling in p65 translocation to the nucleus (Fig. 4). Other reports (Takuwa et al., 1995; Ichikawa and Kiyohara, 2001) have demonstrated that the increase in calcium is dependent on both calcium influx through plasma membrane channels and on calcium release from internal stores. In order to investi-

gate the precise role of the calcium increase in response to serum stimulation, we initially used calcium chelation by BAPTA (Fig. 4 B). Subsequently, the use of flash photolysis for the transient release of the calcium chelator Diazo-2 allowed us to inhibit the serum-induced calcium increase without inhibiting other calcium-dependent events in the cell. Control experiments showed that the uncaging approach was specific and noninvasive. First, illumination was not toxic (cell survival was observed in three independent fields of ∼20 illuminated cells, 20 h after illumination; unpublished data). Second, the inhibitory effect on NF-κB and CD1 promoter activation was dependent on both illumination and on Diazo-2 loading into the cells. Third, the illumination was only effective when it was performed within a few seconds after serum addition to the cells. Uncaging of Diazo-2 before or >1 min after serum stimulation had no inhibitory effect (Fig. S1). Therefore, these control experiments showed that only the precise experimental conditions that led to ablation of the initial calcium peak were able to inhibit subsequent NF-κB activation and CD1 transcriptional activity.

We investigated whether a calcium-dependent protein might activate NF-κB in response to serum. The role of calmodulin, CaMKs, and phosphatase (calcineurin) on IKK/IκB/NF-κB activity has been widely reported in different cell models (Antonsson et al., 2003; Lilienbaum and Israel, 2003), and they were therefore candidate enzymes for transducing the serum-induced calcium signal. CaMKs and calcineurin have also been reported to exert an important role in cell cycle progression (for review see Means, 1994; Santella, 1998). Because CaMKIV is not expressed in Swiss 3T3 fibroblasts (unpublished data), we tested the role of CaMKII by inhibiting its activity with the well-characterized pharmacological inhibitor KN93. This inhibitor had no significant effect on serum-induced NF-κB–luc transcription (Fig. S2). We also saw no significant effect with the calcineurin inhibitor cyclosporin A on serum-induced NF-κB–luc transcription in Swiss 3T3 fibroblasts (Fig. S2). It is notable that most of the previous papers on the relationship between these calcium effector proteins and cell cycle progression report a determinant role of calcium in later stages of the cell cycle, such as the G1/S transition (Takuwa et al., 1995) or the G2/M transition (Patel et al., 1999), rather than at the G0–G1 transition. Therefore, we suggest that in early stages of the cell cycle, CaMKII or calcineurin may not be the main effectors for the regulation of CD1 transcription.

We have demonstrated for the first time the essential role of calcium in the regulation of CD1 transcription and for commitment to cell cycle progression. We found that the early activated mitogenic p42/p44^{MAPK} is calcium sensitive (Fig. 7 A), and that in absence of the calcium signal there was no activation of the NF-κB pathway (IKK phosphorylation, IκBα phosphorylation, and degradation) or subsequent NF-κB–dependent gene transcription. A calcium increase induced by uncaging of caged calcium donor was unable to promote p65 translocation (Fig. 6) and downstream gene transcription (unpublished data). One possible explanation for this would be that the induced calcium increase had a different subcellular localization or dynamics compared to that induced by serum. However, we felt that it was more likely that the coactivation of another upstream pathway by growth factors is

needed for NF-κB activation. Present data suggest that the MAPK cascade is therefore a good candidate for this role.

In conclusion, this study of the kinetics of signaling and transcription in living cells allowed us to understand the critical role of an early transient event (the serum-induced calcium increase) and its later consequences for the fate of the cells. We used state-of-the-art multiparameter noninvasive imaging techniques to follow different biological processes occurring in different time domains from seconds to minutes and hours in the same cells. We propose that the G0–G1 transition is dependent on both mitogenic kinase activity and on calcium signaling. NF-κB activation was also shown to have a critical role in the transduction of these mitogenic signals to the nucleus.

Materials and methods

Reagents and antibodies
Tissue culture medium was from GIBCO BRL; FCS from Harlan Seralab; pharmacological inhibitors Bay117082, PD98059, wortmannin, and BAPTA-AM from Calbiochem; propidium iodide and ribonuclease A from Sigma-Aldrich; and Fluo-4, NP-EGTA, and Diazo-2 from Molecular Probes, Inc.

Antibodies to p65, IκBα, and phospho-Akt (ser 473) and phospho-p42/p44^{MAPK} (Thr185/202/Tyr185/204) were from Cell Signaling Technology, Inc.; anti-actin from Oncogene Research Products; HRP anti–rabbit from Cell Signaling Technology, Inc.; and anti–mouse from Amersham Biosciences.

Cell culture
Swiss albino 3T3 cells were grown in DME supplemented with 10% FCS (vol/vol) and 2 mM L-glutamate at 37°C and 5% CO$_2$. Cells (between passages 6 to 15) were plated at 10^5 cells/ml and were serum starved (0.1% FCS [vol/vol]) 1 d after plating. 10% (vol/vol) serum stimulation was performed 24 h after starvation.

Gene transfer
Plasmids. The pNF-κB-luc construct (Stratagene) contains five repeats of the NF-κB consensus sequence upstream of the luciferase reporter. The CD1-luc reporter plasmids were a gift from Dr. R. Pestell (Albert Einstein College of Medicine, Bronx, NY; Albanese et al., 1995). p65-ds-Red and IκB-EGFP were described previously (Nelson et al., 2002a). The truncated IκBα (missing the 40 NH$_2$-terminal amino acids) was cloned into the pIRES2-EFGP vector (CLONTECH Laboratories, Inc.) and was from Dr. E Costello (University of Liverpool, Liverpool, UK). Plasmids expressing the transdominant-negative IKKα and β were a gift from Dr. N. Inohara (University of Michigan Medical School, Ann Arbor, MI; Tang et al., 2003).

Transfection. Cells were transfected using FuGENE™-6 (Roche) according the manufacturer's instructions.

Microplate luminescence assay
The cells were plated in 24-well plates and transfected on the same day in presence of serum. After 24 h of serum starvation, the cells were treated for 6 h as described in the figure legends. Cell lysis and luminescence measurements were performed as described previously (Nelson et al., 2002b), using a plate reader (LUMIstar; BMG Lab Technologies). The experiments were performed in triplicate.

Live-cell imaging of the luminescent reporter gene
The cells were plated onto 35-mm glass coverslip culture dishes (Iwaki), transfected with the reporter gene, and subsequently serum starved for 24 h. The cells were then incubated on the microscope stage for 2 h at 37°C, 5% CO$_2$, in the presence of 1 mM luciferin (Biosynth AG) and were stimulated with 10% serum. Imaging was carried out using a microscope (Axiovert 100; Carl Zeiss MicroImaging, Inc.) with a Fluar 20×/0.75 NA objective. The photons emitted were collected using a CCD camera (Orca II; Hamamatsu Corporation) cooled to −50°C. A series of images was acquired using a 30-min integration time over a period of 24 h. AQM2000 software (Kinetic Imaging) was used for image acquisition and analysis. For background correction of luminescence images, Lucida version 6 software (Kinetic Imaging) was used to determine the darkest pixel from a comparison of two running consecutive images. Subsequently, a control back-

ground image (processed in the same way) was subtracted from each resulting time point. This allowed for the removal of random noise, cosmic ray events, dark current, and hot pixels. All these experiments were performed at least four times, and in each experiment 5–10 cells were recorded and analyzed.

Fluorescence microscopy
Transfected cells in 35-mm glass coverslip culture dishes (Iwaki) were observed by confocal microscopy using a microscope (LSM510; Carl Zeiss MicroImaging, Inc.) with an F-FLUAR 40×/1.3 NA oil immersion objective. Excitation of EGFP was performed using an argon ion laser at 488 nm. Emitted light was detected through a 505–550-nm bandpass filter from a 545-nm dichroic mirror. dsRed fluorescence was excited using a green helium-neon laser (543 nm) and was detected through both a 545-nm dichroic mirror and a 560-nm long-pass filter. Data capture and extraction was carried out with LSM510 version 3 software (Carl Zeiss MicroImaging, Inc.) using tracking mode to exclude fluorescence cross talk. For the NF-κB–EGFP fusion protein, mean fluorescence intensities were extracted for cells at each time point for both nucleus and cytoplasm. Nuclear/cytoplasmic fluorescence intensity ratios were determined from these data. Concomitantly, the mean cellular fluorescence intensities of IκBα-EGFP fusion proteins were extracted, and the fluorescence intensity relative to starting fluorescence was determined for each cell. All these experiments were performed at least five times, and each time four different fields, which each contained 3–5 transfected cells, were analyzed.

Flow cytometric analysis
After serum stimulation, Swiss 3T3 cells cultured in 25-cm^2 flasks were detached as a single cell suspension with 900 μl trypsin. The cells were stained by addition of 250 μl of 50 μg/ml propidium iodide, 0.15% Triton X-100, and 150 μg/ml RNase A before analysis in an Altra flow cytometer (Beckman Coulter).

Calcium measurement
$[Ca^{2+}]_i$ levels in living 3T3 cells were monitored by fluorescence microscopy using the Ca^{2+} indicator Fluo-4. Cells in 35-mm glass coverslip culture dishes (Iwaki) were incubated at 37°C for 20 min with the acetoxymethyl ester of Fluo-4 (1 μM Fluo-4-AM). After washing off the excess dye, Fluo-4–loaded cells were visualized with an F-Fluar 40×/1.3 NA oil immersion objective. It was observed by time-lapse fluorescence confocal microscopy that prolonged incubation with the fluorochrome led to a punctuate distribution of the dye within the cells.

Flash photolysis
3T3 cells were loaded with the cell permeant acetoxy-methyl ester derivative fluorescent indicator Fluo-4 (0.7 μM) and the caged calcium compound nitro-phenyl-NP-EGTA (NP-EGTA; 0.7μM; Ellis-Davies and Kaplan, 1994) or Diazo-2 (Lannergren and Arner, 1992; Molecular Probes, Inc.).

Photo-release of the caged compounds was induced by a train of 4-μs flashes over a period of 10 s using 360-nm light from a micropoint photoactivation system (Photonic Instruments, Inc.)

RNA extraction and RT-PCR
Total RNA was extracted by using the RNeasy kit (QIAGEN), following the manufacturer's instructions. 2 μg of RNA was used to perform reverse transcriptase PCR (using 200 U M-MLV reverse transcriptase; Promega). For PCR amplification, 5 μl of RT products were incubated with 20 pmol of specific primers and 1 U of Taq DNA polymerase (Promega). PCR products were resolved by agarose gel electrophoresis and were visualized by staining with ethidium bromide. The primers designed with primer 3 software (Rozen and Skaletsky, 2000) were as follows: CD1: 5′-ATGCTGGTTTTTGC-CTGAAG-3′, 5′-TTGTCCCCAATCTCCTTGTC-3′; cyclophilin A: 5′-GTG-GTCTTTGGGAAGGTGAA-3′, 5′-TTACAGGACATTGCGAGCAG-3′.

Western blot analysis
20 μg of total cell extract in sample buffer (62.5 mM Tris HCl, pH 6.8, 10% [vol/vol] glycerol, 1% SDS, 1% [vol/vol] mercaptoethanol, 0.1% bromophenol blue, and protease inhibitor cocktail [Sigma-Aldrich]) was loaded onto a 10% SDS-polyacrylamide gel. For nuclear extracts, cells cultured on 10-cm Petri dishes were washed once with PBS 1×, and scraped in 400 μl of 0.3 M sucrose in AT buffer (AT buffer: 10 mM Tris HCl, pH 8.0, 3 mM CaCl$_2$, 2 mM MgCl$_2$, 0.5 mM DTT, 0.15% [vol/vol], and Triton X-100) and were carefully layered on 400 μl 0.4 M sucrose in AT buffer. After centrifugation at 600 g (for 10 min at 4°C), the pellet was washed once with ice-cold pellet buffer (50 mM Tris HCl, pH 8.0, 1 mM

DTT, 0.2 mM EDTA, and 0.5 mM PMSF) and resuspended in 20 μl pellet buffer, before SDS-PAGE. A Bradford assay was performed before loading to determine the protein concentration. Polypeptides separated by SDS-PAGE were blotted onto a nitrocellulose membrane (0.22 μm; Bio-Rad Laboratories). Blocking and antibody incubations were performed as already described (Sée et al., 2001). The specific bands were detected by ECL (West Pico; Pierce Chemical Co.). Blots were exposed to BIOMAX-MR KODAK films. All Western blot analyses were performed at least three times.

Online supplemental material
Fig. S1 shows controls for photoactivation of the calcium chelator Diazo-2. Fig. S2 shows effects of CaMKII and calcineurin inhibitors on serum-induced NF-κB–dependent transcription. Fig. S3 shows the effect of siRNA knockdown of p65 on serum-induced CD1 transcription. Fig. S4 shows the effect of BAPTA, PD98059, and wortmannin on p-IKK and p-IκBα levels and the effect of PD98059 on IκBα degradation and p65 translocation. Video 1 shows p65 translocation into the nucleus and IκBα degradation after 10% FCS stimulation.

References

Albanese, C., J. Johnson, G. Watanabe, N. Eklund, D. Vu, A. Arnold, and R.G. Pestell. 1995. Transforming p21ras mutants and c-Ets-2 activate the cyclin D1 promoter through distinguishable regions. *J. Biol. Chem.* 270:23589–23597.

Albanese, C., K. Wu, M. D'Amico, C. Jarrett, D. Joyce, J. Hughes, J. Hulit, T. Sakamaki, M. Fu, A. Ben-Ze'ev, et al. 2003. IKKα regulates mitogenic signaling through transcriptional induction of cyclin D1 via Tcf. *Mol. Biol. Cell.* 14:585–599.

Antonsson, A., K. Hughes, S. Edin, and T. Grundstrom. 2003. Regulation of c-Rel nuclear localization by binding of Ca^{2+}/calmodulin. *Mol. Cell. Biol.* 23:1418–1427.

Baeuerle, P.A., and D. Baltimore. 1996. NF-κB: ten years after. *Cell.* 87:13–20.

Baldwin, A.S., Jr. 1996. The NF-κB and IκB proteins: new discoveries and insights. *Annu. Rev. Immunol.* 14:649–683.

Baldwin, A.S., Jr., J.C. Azizkhan, D.E. Jensen, A.A. Beg, and L.R. Coodly. 1991. Induction of NF-κB DNA-binding activity during the G0-to-G1 transition in mouse fibroblasts. *Mol. Cell. Biol.* 11:4943–4951.

Barth, T.F., H. Dohner, C.A. Werner, S. Stilgenbauer, M. Schlotter, M. Pawlita, P. Lichter, P. Moller, and M. Bentz. 1998. Characteristic pattern of chromosomal gains and losses in primary large B-cell lymphomas of the gastrointestinal tract. *Blood.* 91:4321–4330.

Bravo, R. 1990. Genes induced during the G0/G1 transition in mouse fibroblasts. *Semin. Cancer Biol.* 1:37–46.

Brondello, J.M., F.R. McKenzie, H. Sun, N.K. Tonks, and J. Pouyssegur. 1995. Constitutive MAP kinase phosphatase (MKP-1) expression blocks G1 specific gene transcription and S-phase entry in fibroblasts. *Oncogene.* 10:1895–1904.

Brownell, E., H.P. Fell, P.W. Tucker, A.H. Geurts van Kessel, A. Hagemeijer, and N.R. Rice. 1988. Regional localization of the human c-rel locus using translocation chromosome analysis. *Oncogene.* 2:527–529.

Chapman, N.R., G.A. Webster, P.J. Gillespie, B.J. Wilson, D.H. Crouch, and N.D. Perkins. 2002. A novel form of the RelA nuclear factor κB subunit is induced by and forms a complex with the proto-oncogene c-Myc. *Biochem. J.* 366:459–469.

Chen, R.H., C. Sarnecki, and J. Blenis. 1992. Nuclear localization and regulation of erk- and rsk-encoded protein kinases. *Mol. Cell. Biol.* 12:915–927.

Cheng, G., B.F. Liu, Y. Yu, C. Diglio, and T.H. Kuo. 1996. The exit from G$_0$ into the cell cycle requires and is controlled by sarco(endo)plasmic reticulum Ca^{2+} pump. *Arch. Biochem. Biophys.* 329:65–72.

Coqueret, O. 2002. Linking cyclins to transcriptional control. *Gene.* 299:35–55.

Davies, M.A., D. Koul, H. Dhesi, R. Berman, T.J. McDonnell, D. McConkey,

W.K. Yung, and P.A. Steck. 1999. Regulation of Akt/PKB activity, cellular growth, and apoptosis in prostate carcinoma cells by MMAC/PTEN. *Cancer Res.* 59:2551–2556.

Dolmetsch, R.E., K. Xu, and R.S. Lewis. 1998. Calcium oscillations increase the efficiency and specificity of gene expression. *Nature.* 392:933–936.

Ellis-Davies, G.C., and J.H. Kaplan. 1994. Nitrophenyl-EGTA, a photolabile chelator that selectively binds Ca^{2+} with high affinity and releases it rapidly upon photolysis. *Proc. Natl. Acad. Sci. USA.* 91:187–191.

Gilmore, T.D. 1999. Multiple mutations contribute to the oncogenicity of the retroviral oncoprotein v-Rel. *Oncogene.* 18:6925–6937.

Guttridge, D.C., C. Albanese, J.Y. Reuther, R.G. Pestell, and A.S. Baldwin Jr. 1999. NF-κB controls cell growth and differentiation through transcriptional regulation of cyclin D1. *Mol. Cell. Biol.* 19:5785–5799.

Hinz, M., D. Krappmann, A. Eichten, A. Heder, C. Scheidereit, and M. Strauss. 1999. NF-κB function in growth control: regulation of cyclin D1 expression and G0/G1-to-S-phase transition. *Mol. Cell. Biol.* 19:2690–2698.

Ichikawa, J., and T. Kiyohara. 2001. Suppression of EGF-induced cell proliferation by the blockade of Ca^{2+} mobilization and capacitative Ca^{2+} entry in mouse mammary epithelial cells. *Cell Biochem. Funct.* 19:213–219.

Joyce, D., B. Bouzahzah, M. Fu, C. Albanese, M. D'Amico, J. Steer, J.U. Klein, R.J. Lee, J.E. Segall, J.K. Westwick, et al. 1999. Integration of Rac-dependent regulation of cyclin D1 transcription through a nuclear factor-κB-dependent pathway. *J. Biol. Chem.* 274:25245–25249.

Katoch, S.S., X. Su, and R.S. Moreland. 1999. Ca^{2+}- and protein kinase C-dependent stimulation of mitogen-activated protein kinase in detergent-skinned vascular smooth muscle. *J. Cell. Physiol.* 179:208–217.

Lannergren, J., and A. Arner. 1992. Relaxation rate of intact striated muscle fibres after flash photolysis of a caged calcium chelator (diazo-2). *J. Muscle Res. Cell Motil.* 13:630–634.

Lau, L.F., and D. Nathans. 1985. Identification of a set of genes expressed during the G0/G1 transition of cultured mouse cells. *EMBO J.* 4:3145–3151.

Lavoie, J.N., G. L'Allemain, A. Brunet, R. Muller, and J. Pouyssegur. 1996. Cyclin D1 expression is regulated positively by the p42/p44^{MAPK} and negatively by the p38/HOG^{MAPK} pathway. *J. Biol. Chem.* 271:20608–20616.

Lee, R.J., C. Albanese, R.J. Stenger, G. Watanabe, G. Inghirami, G.K. Haines III, M. Webster, W.J. Muller, J.S. Brugge, R.J. Davis, and R.G. Pestell. 1999. pp60^{v-src} induction of cyclin D1 requires collaborative interactions between the extracellular signal-regulated kinase, p38, and Jun kinase pathways. A role for cAMP response element-binding protein and activating transcription factor-2 in pp60^{v-src} signaling in breast cancer cells. *J. Biol. Chem.* 274:7341–7350.

Lenormand, P., C. Sardet, G. Pages, G. L'Allemain, A. Brunet, and J. Pouyssegur. 1993. Growth factors induce nuclear translocation of MAP kinases (p42^{mapk} and p44^{mapk}) but not of their activator MAP kinase kinase (p45^{mapkk}) in fibroblasts. *J. Cell Biol.* 122:1079–1088.

Lilienbaum, A., and A. Israel. 2003. From calcium to NF-κB signaling pathways in neurons. *Mol. Cell. Biol.* 23:2680–2698.

Madrid, L.V., M.W. Mayo, J.Y. Reuther, and A.S. Baldwin Jr. 2001. Akt stimulates the transactivation potential of the RelA/p65 Subunit of NF-κB through utilization of the IκB kinase and activation of the mitogen-activated protein kinase p38. *J. Biol. Chem.* 276:18934–18940.

Matsumura, I., T. Kitamura, H. Wakao, H. Tanaka, K. Hashimoto, C. Albanese, J. Downward, R.G. Pestell, and Y. Kanakura. 1999. Transcriptional regulation of the cyclin D1 promoter by STAT5: its involvement in cytokine-dependent growth of hematopoietic cells. *EMBO J.* 18:1367–1377.

McNeil, P.L., M.P. McKenna, and D.L. Taylor. 1985. A transient rise in cytosolic calcium follows stimulation of quiescent cells with growth factors and is inhibitable with phorbol myristate acetate. *J. Cell Biol.* 101:372–379.

Means, A.R. 1994. Calcium, calmodulin and cell cycle regulation. *FEBS Lett.* 347:1–4.

Meng, F., L. Liu, P.C. Chin, and S.R. D'Mello. 2002. Akt is a downstream target of NF-κB. *J. Biol. Chem.* 277:29674–29680.

Nelson, G., L. Paraoan, D.G. Spiller, G.J. Wilde, M.A. Browne, P.K. Djali, J.F. Unitt, E. Sullivan, E. Floettmann, and M.R. White. 2002a. Multi-parameter analysis of the kinetics of NF-κB signalling and transcription in single living cells. *J. Cell Sci.* 115:1137–1148.

Nelson, G., G.J. Wilde, D.G. Spiller, E. Sullivan, J.F. Unitt, and M.R. White. 2002b. Dynamic analysis of STAT6 signalling in living cells. *FEBS Lett.* 532:188–192.

Ozes, O.N., L.D. Mayo, J.A. Gustin, S.R. Pfeffer, L.M. Pfeffer, and D.B. Donner. 1999. NF-κB activation by tumour necrosis factor requires the Akt serine-threonine kinase. *Nature.* 401:82–85.

Pages, G., P. Lenormand, G. L'Allemain, J.C. Chambard, S. Meloche, and J. Pouyssegur. 1993. Mitogen-activated protein kinases p42^{mapk} and p44^{mapk} are required for fibroblast proliferation. *Proc. Natl. Acad. Sci. USA.* 90:8319–8323.

Patel, R., M. Holt, R. Philipova, S. Moss, H. Schulman, H. Hidaka, and M. Whitaker. 1999. Calcium/calmodulin-dependent phosphorylation and activation of human Cdc25-C at the G2/M phase transition in HeLa cells. *J. Biol. Chem.* 274:7958–7968.

Rayet, B., and C. Gelinas. 1999. Aberrant rel/nfkb genes and activity in human cancer. *Oncogene.* 18:6938–6947.

Rocha, S., A.M. Martin, D.W. Meek, and N.D. Perkins. 2003. p53 represses cyclin D1 transcription through down regulation of Bcl-3 and inducing increased association of the p52 NF-κB subunit with histone deacetylase 1. *Mol. Cell. Biol.* 23:4713–4727.

Romashkova, J.A., and S.S. Makarov. 1999. NF-κB is a target of AKT in anti-apoptotic PDGF signalling. *Nature.* 401:86–90.

Romieu-Mourez, R., D.W. Kim, S.M. Shin, E.G. Demicco, E. Landesman-Bollag, D.C. Seldin, R.D. Cardiff, and G.E. Sonenshein. 2003. Mouse mammary tumor virus c-rel transgenic mice develop mammary tumors. *Mol. Cell. Biol.* 23:5738–5754.

Rozen, S., and H.J. Skaletsky. 2000. Primer3 on the WWW for general users and for biologist programmers. *Methods Mol. Biol.* 132:365–386.

Ryan, K.M., M.K. Ernst, N.R. Rice, and K.H. Vousden. 2000. Role of NF-κB in p53-mediated programmed cell death. *Nature.* 404:892–897.

Santella, L. 1998. The role of calcium in the cell cycle: facts and hypotheses. *Biochem. Biophys. Res. Commun.* 244:317–324.

See, V., A.L. Boutillier, H. Bito, and J.P. Loeffler. 2001. Calcium/calmodulin-dependent protein kinase type IV (CaMKIV) inhibits apoptosis induced by potassium deprivation in cerebellar granule neurons. *FASEB J.* 15:134–144.

Sen, R., and D. Baltimore. 1986. Inducibility of kappa immunoglobulin enhancer-binding protein Nf-κB by a posttranslational mechanism. *Cell.* 47:921–928.

Takuwa, N., W. Zhou, M. Kumada, and Y. Takuwa. 1995. Involvement of intact inositol-1,4,5-trisphosphate-sensitive Ca^{2+} stores in cell cycle progression at the G1/S boundary in serum-stimulated human fibroblasts. *FEBS Lett.* 360:173–176.

Tang, E.D., N. Inohara, C.Y. Wang, G. Nunez, and K.L. Guan. 2003. Roles for homotypic interactions and transautophosphorylation in IκB kinase β (IKKβ) activation. *J. Biol. Chem.* 278:38566–38570.

Thanos, D., and T. Maniatis. 1995. NF-κB: a lesson in family values. *Cell.* 80:529–532.

Truneh, A., F. Albert, P. Golstein, and A.M. Schmitt-Verhulst. 1985. Early steps of lymphocyte activation bypassed by synergy between calcium ionophores and phorbol ester. *Nature.* 313:318–320.

Watanabe, G., C. Albanese, R.J. Lee, A. Reutens, G. Vairo, B. Henglein, and R.G. Pestell. 1998. Inhibition of cyclin D1 kinase activity is associated with E2F-mediated inhibition of cyclin D1 promoter activity through E2F and Sp1. *Mol. Cell. Biol.* 18:3212–3222.

Westerheide, S.D., M.W. Mayo, V. Anest, J.L. Hanson, and A.S. Baldwin Jr. 2001. The putative oncoprotein Bcl-3 induces cyclin D1 to stimulate G_1 transition. *Mol. Cell. Biol.* 21:8428–8436.

Whitaker, M., and M.G. Larman. 2001. Calcium and mitosis. *Semin. Cell Dev. Biol.* 12:53–58.